Optimal Operation of Interconnected Energy Hubs by Using Decomposed Hybrid Particle Swarm and Interior-Point Approach

Da Huo, Simon Le Blond, Chenghong Gu, Wei Wei, and Dongmin Yu

dh466@bath.ac.uk, University of Bath

***Abstract*—The Energy Hub has become an important concept for formally optimizing multi-carrier energy infrastructure to increase system flexibility and efficiency. The existence of energy storage within energy hubs enables the dynamic coordination of energy supply and demand against varying energy tariffs and local renewable generation to save energy cost. The battery lifetime cost may be included in the optimization objective function to better utilize battery for long term use. However, the operational optimization of an interconnected energy hub system with battery lifetime considered presents a highly constrained, multi-period, non-convex problem. This paper proposes Particle Swarm Optimization (PSO) hybridised with a numerical method, referred to collectively as the decomposed approach. It decouples the complicated optimization problem into sub-problems, namely the scheduling of storage and other elements in the energy hub system, and separately solves these by PSO and the numerical method 'interior-point'. This approach thus overcomes the disadvantages of numerical methods and artificial intelligence algorithms that suffer from convergence only to a local minimum or prohibitive computation times, respectively. The new approach is applied to an example two-hub system and a three-hub system over a time horizon of 24 hours. It is also applied to a large eleven-hub system to test the performance of the approach and discuss the potential applications. The results demonstrate that the method is capable of achieving very near the global minimum, verified by an analytical approach, and is fast enough to allow an online, receding time horizon implementation.**

***Index Terms*—Energy hub, energy sharing, energy storage, multi-period optimization, particle swarm optimization.**

I. Introduction

Energy hub modelling relates to the utilization of co-generation or tri-generation, which increases system flexibility by means of exploiting every available energy carrier, such as electricity, gas, and heat [1, 2]. A typical energy hub contains multiple energy carriers, which achieves the function of importing, exporting, converting, and storing energy [3, 4]. The energy hub approach takes advantage of existing infrastructures as much as possible and can be applied to various sizes of the energy system. Domestic buildings are modelled in this paper, which consume approximately 40% of society's total energy [5] but an individual domestic load profile is fairly stochastic such that it cannot always be met with onsite generation. Interconnecting heterogeneous energy infrastructure at local level can best leverage renewable generation and pooled storage without suffering large distance transmission losses and enable self-sufficient energy communities.

The optimal operation of an energy hub system enables the effective utilization of the elements within the system to minimise energy use, monetary cost or emissions, or some weighted combination of these objectives. Different algorithms have been applied to the multi-hub optimization problem. Reference [6] presents a decomposed solution of a multi-agent genetic algorithm to optimize the power and gas flow between energy hubs. Papers [7] and [8] employ model predictive control (MPC) to optimally control the operation of three interconnected energy hubs, although numerical methods are applied within the MPC scheme, so a global minimum cannot be guaranteed in the solution. In [9] and [10], a grid of 10 hubs is modelled, where the energy transfer between hubs is formulated as a non-cooperative game. The existence of the unique Nash equilibrium is proved. References [11, 12] propose an integrated demand response program and simulate the scheme on a smart grid of six energy hubs. The integrated demand response problem is formulated as an ordinal potential game and the Nash equilibrium is proven to be unique. Reference [13] investigates the performance of an energy management system under different energy pricing schemes for a group of 10 hubs. Reference [14] introduces the "smart energy hub" system which uses a cloud computing platform to enable customers with must run loads to participate in a demand side management program. Reference [15] investigates the optimization performance between deterministic and stochastic approaches applied to multi-period optimization for a 3-hub system over a mixed industrial and residential area. Reference [16] generates a novel mathematical model for storage, general appliances, and other renewable components in residential houses. Mixed integer linear programming (MILP) is applied to optimize the control for residential energy hubs considering end-user preferences.

References [9] to [15] propose the optimization for multi-hubs. However, storage is not considered when the problem is formulated as a non-convex problem in [9] to [12]. In reference [13], the storage is modelled in the energy hub optimization, but the problem is formulated as a convex problem. The optimal operation of multiple hubs with energy storage and interconnection available between hubs has hitherto been formulated as a highly constrained, non-linear multi-period

optimization. However, the lifetime of the battery system suffers as its utilization increases, an aspect which has not been addressed in previous energy hub literature. In this paper, the battery lifetime cost is calculated and included in the objective function based on the method proposed by [17]. Therefore, the optimization problem is formulated as a non-convex, multi-period problem.

Numerical algorithms such as MILP provide fast computation times, but perform poorly when solving non-convex problems, because the solver can easily fall into local minima. Alternatively, particle swarm optimization (PSO) and related optimization approaches have been applied to optimize the operation of power systems due to their straightforward implementation and high efficiency [18]. For example, multi-pass iteration PSO was applied to the optimal scheduling of a battery coupled with wind turbine generators [19]. Co-evolutionary PSO was applied to smart home operation strategies [20]. A hybrid algorithm combining PSO and a bacterial foraging algorithm was proposed and applied to the optimal scheduling of an active distribution network [21].

Despite high robustness and accuracy compared with other algorithms [19], PSO has never been applied to solve energy hub optimization problems. However, conventional PSO is not suitable for solving highly-constrained non-linear problems with a large number of variables where the feasible region is narrow in hundreds of dimensions, meaning the time spent on finding feasible particles is considerable. Thus, improvement to conventional PSO is required in order to fully harness its potential for multi-hub optimization. This paper proposes a decomposed solution by applying a novel hybrid PSO and numerical optimization by combining conventional PSO with the 'interior point' method. Each particle in the PSO routine represents the storage operations over the whole optimization time horizon (24 hours in this paper). Based on the storage operation, the 'interior-point' algorithm is applied to optimize the operations of other elements in the system of energy hubs over 24 hours. The resulting energy cost over the full 24 hour time horizon is formulated as the fitness score. All particles then are updated based on the conventional PSO routine until the optimization completes. The decomposed approach is demonstrated to be capable of optimizing multi-energy hubs efficiently, and the storage operation obtained from the decomposed approach is benchmarked to be very close to the theoretical optimal strategy of storage. Additionally, the decomposed PSO yields better optimization results with less computation compared with the conventional PSO. The approach is applied to two energy hub systems to illustrate its effectiveness. The main contributions of this paper are illustrated as follows:

i) A decomposed approach of applying particle swarm optimization is proposed in this paper, and it is capable of solving the non-convex multi-period optimization problem. The decomposed approach is validated by a simple two-hub system for which the theoretical minimum can be derived empirically.

ii) A group of residential houses is simulated as an interconnected energy hub system, an optimization problem is expressed to minimize the total cost of the energy hub system over 24 hours. With the battery lifetime cost considered in the optimization, the problem is formulated as a non-convex problem. The decomposed PSO approach is applied to optimally solve the problem. The optimization results indicate that the battery SOC varies between 60% and 90% to avoid unnecessary degradation of the battery lifetime for three residential hubs.

iii) The performance of the decomposed PSO approach is compared with the conventional PSO being applied to solve a same three-hub problem. The decomposed approach achieves a 58% greater energy saving for three-hub optimization with 98% saving of computation time comparing with the conventional PSO.

This paper is organized in six sections. Section II illustrates the general optimization problems for multi-energy hubs which the energy interconnection is enabled between hubs. An explicit description of the decomposed approach applying PSO is presented in section III. Section IV presents the case studies and related results. Section V concludes the paper.

II. Energy Hub Optimization

A. Energy hub modelling

A typical energy hub model that enables energy sharing between hubs is shown in Fig. 1. It consumes various input resources including electricity from grid (P_{ele}), solar energy (P_{so}), and gas (P_{gas}) to meet the electricity load (L_{ele}) and thermal load (L_{th}). The energy flow between hubs is denoted by E_{rh} and H_{rh} , which indicate the power and heat exchange with other hubs. The mathematical formulation between hub inputs and outputs under steady state operation is shown in (1).

$$\begin{bmatrix} L_{ele}(t) \\ L_{th}(t) + H_{rh}(t) \end{bmatrix} = \begin{bmatrix} \eta_{PV}\cdot(1-\nu_1(t)) & 1-\nu_1(t) & \nu_2(t)\cdot\eta_e \\ \eta_{PV}\cdot\nu_1(t)\cdot CoP & \nu_1(t)\cdot CoP & \nu_2(t)\cdot\eta_{th}+\eta_{bo}\cdot(1-\nu_2(t)) \end{bmatrix} \times \begin{bmatrix} P_{so}(t) \\ P_{ele}(t) + E_{sh}(t) - E_{hs}(t) + E_{rh}(t) \\ P_{gas}(t) \end{bmatrix} \quad (1)$$

The first matrix on the right hand side is the coupling matrix C, which defines the relationship between inputs *P* and outputs *L*. The parameter t within the brackets indicates that these variables are time dependent. Since the problem is considered in a discretized time domain, they are fixed in each time step. The coefficient ν is the dispatch factor between 1 and 0 which generally denotes the portion of the energy injected to a certain

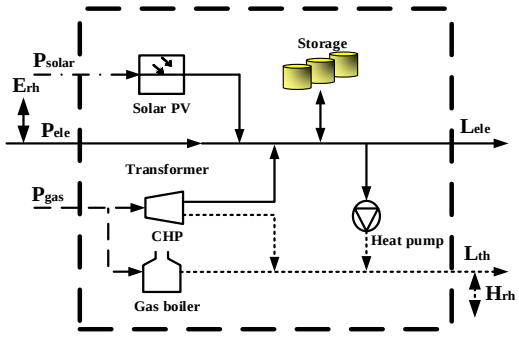

Fig. 1. An example of energy hub model

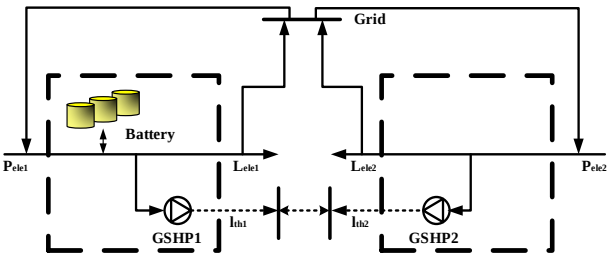

Fig. 2. Two-hub system with energy sharing available between hubs.

converter. For the example energy hub model, υ_1 is the portion of electricity injected to heat pump over total electricity input. υ_2 indicates the percentage of gas input to CHP over total gas input. Parameters η_{so} and η_{bo} express the efficiency of the Solar PV and boiler respectively. η_e and η_{th} represents the electric efficiency and thermal efficiency of CHP respectively. E_{sh} and E_{hs} indicate the charging and discharging energy.

The assumptions for modelling the energy hub system are as follows:

Assumption 1: The energy hub system modelled enables electricity and heat sharing between hubs. The electrical interconnection between hubs is the electricity exchange with the grid. For example, in Fig. 2 electricity transfer from hub 1 to hub 2 is achieved by injecting electricity to grid from hub 1, and extracting the same amount of electricity from grid to hub 2. For heat transfer, a district heat network must be installed between the hubs.

B. Converter modelling

The most common residential heating in the UK, a gas boiler, is modelled within the energy hub. The efficiency of a gas boiler can be formulated as a nonlinear expression in terms of the input energy $P_{gas}(t)$.

Assumption 2: the efficiency of the boiler simulated in this paper is non-constant, and the characteristics of the cyclic fuel utilization efficiency with respect to cyclic input energy normalized by steady-state input energy is derived based on Reference [22]. The data points and approximated curve are shown in Fig. 3.

The boiler efficiency varying with the input energy can, therefore, be represented by the approximated curve. The expression of boiler efficiency η_{bo} is shown in (2):

$$\eta_{bo}(t) = 0.8218646 - 0.01686 \div P^{*}_{gas}(t) \tag{2}$$

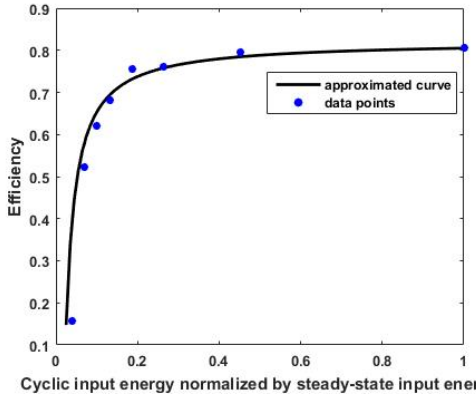

Fig. 3. Boiler efficiency against cyclic input energy normalized by steady-state input energy

Where $P_{gas}{}^{*}(t)$ is the value of instant gas input at time step t normalized by steady-state input.

In addition, the ground source heat pump (GSHP) is selected in this paper due to its high efficiency and potential to decarbonise heat, and its increasing uptake in some European countries, America and Japan [23]. The efficiency of the heat pump is described as the Coefficient of Performance (CoP) and is expressed in (3):

$$\text{Heat output} = \text{CoP} \times \text{P}_{\text{hp}}(t) \tag{3}$$

Where P_{HP} is the power input to the GSHP.

Assumption 3: the CoP of GSHP is set to be constant over the whole time horizon.

Micro-combined heat and power (micro-CHP) reduces electricity utilization from the grid and increases energy efficiency by simultaneously generating power and heat [24]. Hence it is modelled in this paper.

Assumption 4: The micro-CHP simulated in this paper is assumed to be steady-state with constant electric efficiency and thermal efficiency. The ramp rate constraint e_{ramp} to restrict the micro-CHP power output is considered and given by (4), e_p is the power output of the micro-CHP.

$$-e_{ramp} \le e_p(t-1) - e_p(t) \le e_{ramp} \tag{4}$$

C. Energy storage modelling

The lead-acid battery is employed as the energy storage within the energy hubs in this work. The battery is considered to be a simple buffering device. Since the electrical energy within the storage at the current time step is equal to the electricity at last time step plus the charging energy or minus the discharging energy, and minus the standby loss. The i_{th} battery's energy level $E_i(t)$ is mathematically expressed in (5).

$$E_i(t) = E_i(t-1) + E_{stb,i}(t) + E_{hs,i}(t) \times \eta_{char} - E_{sh,i}(t) / \eta_{dis} \tag{5}$$

$E(t-1)$ represents the energy within the storage in the previous time step. E_{stb} is the standby loss, E_{sh} and E_{hs} indicate the charging and discharging energy. η_{char} and η_{dis} are charging efficiency and discharging efficiency respectively. Since the battery can only charge, discharge, or on standby at any time step, constraint (6) is considered in the optimization problem.

$$E_{hs,i}(t) \times E_{sh,i}(t) = 0 \tag{6}$$

In addition, the characteristic of battery lifetime is considered since the operation of the battery at different states of charge (SOC) result in different losses. The lifetime drops quicker when operating the battery during low SOCs compared to high SOCs [25]. To maximize the benefits of battery utilisation from the prospective of long term operation, the battery lifetime cost penalty is calculated and added to the objective function. Reference [17] suggests the method of calculating battery lifetime cost $C_{bl}(t)$ and it is illustrated in Appendix.

Assumption 5: During the process of optimization, the initial state of charge of each battery is set to be 70%, and to consistently utilize the batteries for the next day, the state of charge at the final time step needs to be reverted to above 70%. The SOC of the three batteries is assumed to be limited between 0 and 100%.

D. Optimization problem description

The objective is to minimize the system cost including the energy cost and battery lifetime cost over a time horizon of 24 hours. With the knowledge of electricity load, heat load, energy carrier price and solar energy generation, the objective is to control the energy hub operation at each time step to achieve a holistic 24 hour optimization. The system operation vector contains energy injected into each hub, the dispatch factor within each hub, the energy exchange between hubs, and the charging/discharging energy of energy storage at each time step. The control vector $u(t)$ is expressed in (7):

$$u(t) = \left[P_{ele,i}(t), P_{gas,i}(t), E_{ij}(t), H_{ij}(t), E_{sh}(t), v_i(t)\right], \forall i, \forall t \quad (7)$$

For a system containing Ω number of interconnected energy hubs, the optimization problem may be formulated as equations (8a) to (8o), the variables used in problem (8) are defined thusly:

Subscripts i and j denote the hub index. $P_{ele}(t)$ and $P_{gas}(t)$ represent the electricity and gas input to energy hub at time step t. $v_i(t)$ denotes the dispatch factor at time step t. The electricity and heat exchange between hubs are denoted as $E_{ij}(t)$ and $H_{ij}(t)$, which means the energy flow direction is from hub *i* to hub *j* at time step t. The flow direction is reversed when the value of $E_{ij}(t)$ and $H_{ij}(t)$ are negative. $SOC(t)$ is the battery state of charge. $E_s(t)$ represents the energy stored in the battery at time step t, which has to be limited within the battery capacity. $E_{sh}(t)$ and $E_{hs}(t)$ are the charging and discharging power from the battery. Π(t) denotes the energy price. $P_{HP}(t)$ and $P_{Bo}(t)$ are the energy injection to heat pump and boiler respectively. N is the number of total time steps. $e_p(t)$ represents the electricity output of Micro-CHP, and $e_{ramp}(t)$ is the Micro-CHP ramp rate at time step t.

The optimization problem is described by (8a) – (8o):

Minimize

$$\sum_{t=1}^{N}\left[\sum_{i=1}^{\Omega}\left[P_{ele,i}(t)\times\Pi_{ele}(t)+P_{gas,i}(t)\times\Pi_{gas}(t)+C_{bl,i}(t)\right]\right] \quad (8a)$$

Subject to

$$L_i(t) = C_i(t) \times P_i(t), \forall i, \forall t \quad (8b)$$

$$0 \le v_i(t) \le 1 \ \forall i, \forall t \quad (8c)$$

Electricity

$$P_{ele,i,min}(t) \le P_{ele,i}(t) \le P_{ele,i,max}(t), \forall i, \forall t \quad (8d)$$

$$E_{ij,min}(t) \le E_{ij}(t) \le E_{ij,max}(t), \forall i, \forall t \quad (8e)$$

Heat

$$H_{ij,min}(t) \le H_{ij}(t) \le H_{ij,max}(t), \forall i, \forall t \quad (8f)$$

Battery

$$SOC_{i,min}(t) \le SOC_i(t) \le SOC_{i,max}(t), \forall i, \forall t \quad (8g)$$

$$0 \le E_{sh,i}(t) \le E_{sh,i,max}(t), \forall i, \forall t \quad (8h)$$

$$0 \le E_{hs,i}(t) \le E_{hs,i,max}(t), \forall i, \forall t \quad (8i)$$

$$E_{sh,i}(t) \times E_{hs,i}(t) = 0, \forall i, \forall t \quad (8j)$$

Micro-CHP

$$e_{p,i,min}(t) \le e_{p,i}(t) \le e_{p,i,max}(t), \forall i, \forall t \quad (8k)$$

$$e_{ramp}(t) \le e_{p,i}(t) - e_{p,i}(t-1) \le e_{ramp}(t), \forall i, \forall t \quad (8l)$$

Gas

$$P_{gas,i,min}(t) \le P_{gas,i}(t) \le P_{gas,max}(t), \forall i, \forall t \quad (8m)$$

GSHP

$$P_{HP,i,min}(t) \le P_{HP,i}(t) \le P_{HP,i,max}(t), \forall i, \forall t \quad (8n)$$

Boiler

$$P_{Bo,i,min}(t) \le P_{Bo,i}(t) \le P_{Bo,i,max}(t), \quad \forall i, \forall t \quad (8o)$$

As indicated by (8), the optimization is carried out considering the security constraints. (8b) indicates the coupling between hub input and output, where constraints (2) (3) and (5) are included in (8b), and (1) is the transformation of (8b). (8d) and (8m) refer to the minimum and maximum energy input to a single hub. (8e) and (8f) suggest the adjustment of energy transmission limitation between hubs. (8g) indicates the limitation of energy level within batteries. (8h) and (8i) indicate the limitation of charging energy and discharging energy at each time step. (8j) avoids simultaneously charging and discharging the battery. (8k), (8n), and (8o) represent the minimum and maximum energy injection to micro-CHP, GSHP, and boiler respectively. (8l) limits the ramp rate for micro-CHP electric output.

Whilst solving the energy hub optimization problem, the control variables mentioned in (7) at each time step must satisfy all constraints illustrated above. Therefore, the multi-hub problem is necessarily a multi-period optimization containing a large number of variables and constraints. For instance, the 3-hub scenario investigated in this paper contains 504 variables and 480 constraints. Clearly, the optimization problem becomes more complicated as the number of hubs increases. Additionally, it was concluded by graphing the functions associated with the battery lifetime cost ((A1) to (A6) in the Appendix) that these fail to satisfy the definition of a convex problem, given in Appendix (A7)-(A9), in particular that the resulting objective function failed to satisfy (A9). Therefore, the optimization problem is a non-convex problem.

III. Decomposed PSO

A. PSO

Particle swarm optimization was proposed based on the behaviour of flocking birds or schools of fish [26]. Each particle describes a solution to a problem that can be quantitatively measured by its performance. At each iteration of the optimization, the particles trend towards the global minimum based on two factors, the best performance of any particle ever achieved P_i^g and the best position P_i^k of particle *i*. The PSO working mechanism is illustrated by means of mathematical formulations in (9) and (10):

The position X of a particle i at iteration $k+1$ is

$$X_i^{k+1} = X_i^k + V_i^{k+1} \quad (9)$$

V_i^{k+1} indicates the new velocity for particle i at $k+1$ iteration. It is derived as:

$$V_i^{k+1} = \omega V_i^k + c_1 r_1\left(P_i^k - X_i^k\right) + c_2 r_2\left(P_i^g - X_i^k\right) \quad (10)$$

r_1 and r_2 represent two random numbers between 0 and 1. c_1 and c_2 are the cognitive parameter and social parameter, the

two weighting factors that model the confidence of the current particle in itself and in the swarm [27]. Parameter ω is the inertia weight, a coefficient applied to particle velocity, which influences the PSO convergence behaviour by increasing the distance the particle will travel from its previous position.

At the beginning of the optimization, the PSO algorithm firstly generates a population of particles randomly over the search space, where the position of each particle represents a solution. The particles are evaluated by applying the solution to the problem to obtain a fitness score for each particle. P_i^g and P_i^k can therefore be found. All particles are updated using (9) and (10) at each iteration, with this process repeated until the stopping criteria is met.

When conventional PSO is used on highly constrained and non-convex optimization problems, the particles tend to fall into infeasible regions during initialization and updating. This problem can be solved by utilizing the sequential quadratic programming (SQP) algorithm [28]. The SQP algorithm solves an optimization problem by seeking the Karush-Kuhn-Tucker first order optimally condition, which can find a local minimum near the starting point. In other words, the position of an infeasible particle is taken as the starting point and then by utilizing the SQP algorithm, a feasible particle can be found nearby that replaces the infeasible one.

B. Decomposed approach

The multi-energy hub optimization is a multi-period problem with many variables. Since the main purposes of storage are to time-shift renewably generated energy to meet loads and arbitrage against varying tariffs, its operational management must, therefore, consider the energy price, renewable generation, and converter working status to schedule its operational state in each time step, i.e. charging, discharging or on standby. The operation of storage in the current time step will influence the operation in other time steps and thus a multi-period optimization approach is necessary. The complexity of the problem requires significant computation time and may compromise optimization accuracy. However, if the optimal operation of the complex time-dependent device (such as storage) is known in advance, other control variables in (7) can then be obtained by applying numerical methods in each time step.

The stochastic nature of PSO is capable of solving non-convex problems with non-continuous search spaces, whilst the numerical function 'interior-point' can handle non-linear constrained problems with acceptable performance and computation time, so the decomposed approach here harnesses advantages of both methods. In general, during the generating and updating of all particles, only the control information of every battery is included in each particle (i.e. charging and discharging energy). For the optimization of a three-hub system containing three batteries over 24 time steps, there are totally 144 variables included in each particle. Whilst the operations of remaining elements in the energy hub system are derived using the interior point method based on the information in each particle, and the fitness score of each particle can therefore be calculated. The procedure is shown in Fig. 4 and can be described thusly:

1) Randomly initialize a population of particles, where the position of each particle denotes the solution of two variables over 24 hours: charging energy and discharging energy. The variables should be generated within the boundary set by the optimization, including the maximum charging/discharging energy, minimum and maximum battery capacity or SOC as indicated in (8h), (8i) and (8g). The magnitude of charging power at each step multiplied by discharging power should be equal to zero, meaning the battery can only either be charging, discharging, or on standby. This is achieved by applying SQP algorithm to find a feasible point satisfying above conditions near the initial point.
2) For each time step, the charging and discharging energy can be regarded as the extra output and input for energy hub system without a battery. Therefore, the operations of the battery between each time step can be decoupled from each other.
3) The 'interior-point' method is then applied to optimize the operation over the whole time period based on electricity load, heat load, renewable energy generation, extra input, and extra output. The optimized total system cost over 24 time steps is then derived. Meanwhile, the battery lifetime cost related to the battery working status over 24 time steps is calculated. The fitness score of each particle is thus the total operational cost from both battery operation and optimized overall hub management.

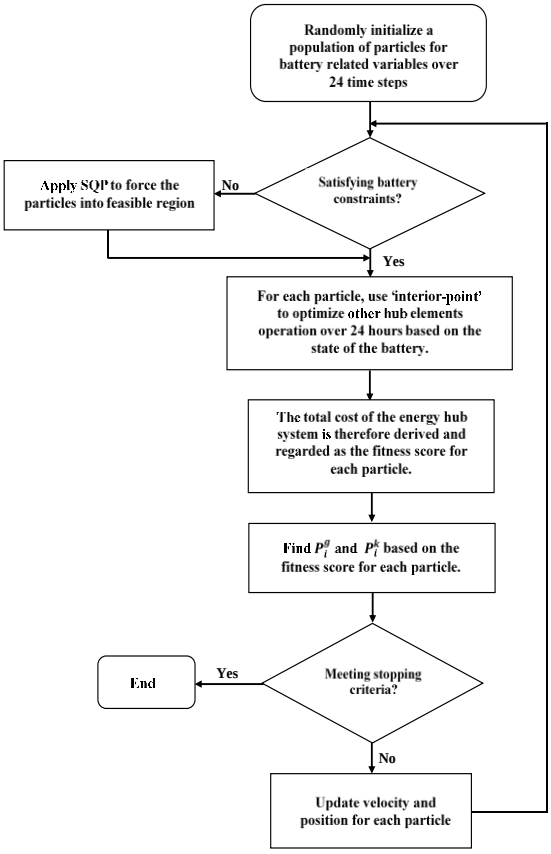

Fig. 4. The working flow of the decomposed approach

4) Find P_i^g and P_i^k, see if the best particle satisfies the stopping criteria. If the stopping criteria is met, then the solution of the best particle is the final solution to the optimization. If not, update the velocities and positions for particles based on (9) and (10).
5) Repeat steps 2 to 4 until the stopping criteria is met.

The decomposed approach decouples the optimization for batteries and other hub elements. The optimal operations of batteries are derived based on the PSO, the optimization for other hub elements is obtained by applying the interior-point method. The efficiency of the algorithm is increased, and the computation time is therefore reduced.

The decomposed-PSO algorithm is achieved based on modification of the open source PSO MATLAB routine developed by ETH Zurich [28]. The decomposed method is illustrated in terms of the optimization for the two-hub system in next section.

IV. Demonstration

This section applies the novel PSO algorithm to two multi energy-hub systems across two use scenarios. The first part introduces a two-hub system, which is simple enough such that a theoretical minimum may be analytically calculated for benchmarking the performance of the PSO algorithm. The second part investigates a three-hub system with converters and batteries illustrated in section II. The potential application of the decomposed approach is discussed based on the computation speed and operation results in the third part.

A. Two-hub System

To demonstrate the effectiveness of the decomposed-optimization in finding the global minimum, a 2-hub system optimization problem is proposed and investigated. The battery lifetime cost is excluded in the problem, hence the theoretical minimum can be derived analytically, and the performance of the decomposed approach can be evaluated. The 2-hub system with energy sharing is shown in Fig. 2.

Each of the two hubs represents a residential house. The load and generation profile is assumed to be a winter day in the UK based on [29] and [30]. A battery is equipped in hub 1, with charging efficiency and discharging efficiency assumed to be 95%, and standby losses assumed to be negligible (justified because the self-discharge rate on diurnal timescales is very small). The battery minimum and maximum capacities are 4 kWh and 17.376 kWh. To verify that the redundant energy within each hub is adequately utilized by the energy sharing between hubs, the different performance of converters is assumed in each hub. A ground source heat pump with CoP of 3.0 and another heat pump with CoP of 4.2 are included in hub 1 and hub 2 respectively. Time-of-use electricity tariffs (derived from [31]) are assumed, in this case shown in Fig. 5. The optimization problem statements refer to (8).

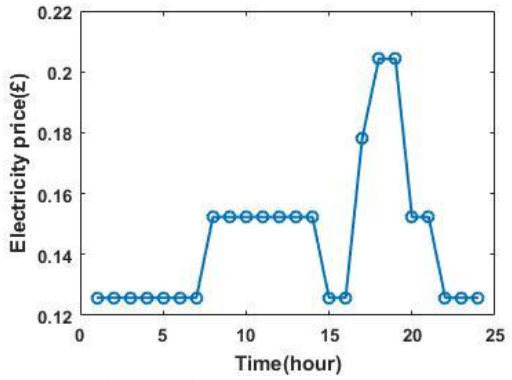

Fig. 5. The time-of-use tariffs against 24 hours.

1) Validation

The benchmark approach to calculate the global minimum of the two-hub system over 24 hours is shown in this section. The total energy cost, *TC*, for the two hubs is given in (11).

$$TC = \sum_{t=1}^{24} \left[P_{ele,1}(t) + P_{ele,2}(t) + E_{sh}(t) \right] \times \Pi_{ele}(t) \tag{11}$$

$P_{ele,1}(t)$ and $P_{ele,2}(t)$ indicate the electricity consumption for hub 1 and hub 2 respectively. $E_{sh}(t)$ represents the electricity exchange between hubs and energy storage. The optimization strategy is as follows: the consumed electricity is utilized to support the ground source heat pump to generate heat, and meet the electricity load. According to equation (3), the electricity requirement for heat can be reduced by exploiting the high CoP of heat pumps. Since heat between hubs is transferable, the heat pump in hub 2 (CoP of 4.2) is applied to support the heat load for two hubs at each time step.

In addition to selecting high performance heating converters, storage can also be utilized to reduce energy cost. Based on achieving the objective of reducing the energy cost for the whole system, the operation of the battery should follow the broad strategy of charging during low tariffs and discharging during high tariffs. The battery needs to be fully charged during periods 1-7 since the electricity prices at these times are lowest. For periods 17-19, the prices are the highest, hence the storage needs to discharge within the maximum discharging power. The price from 15-16 is the lowest, hence some energy could be charged during 8-14 and recharge during 15-16 only if the remaining power at the end of 16 is capable of meeting the demand during 17-19. After considering the maximum

TABLE I
The Optimal Operations for Battery

Period	Charging energy(kWh)	Discharging energy(kWh)	Battery state of charge(kWh)
1-7	14.08	0	17.376
8-14	0	6	11.376
15-16	6	0	17.076
17	0	2.646	14.429
18-19	0	5.78	8.649
20-21	0	4.6494	4
22-24	0	0	4

TABLE II
Optimization Results for 2-Hub System

Particle population	Optimization results(£)	Computation time(s)
10	6.783	106
20	6.776	250
30	6.737	271
40	6.733	260
50	6.752	419

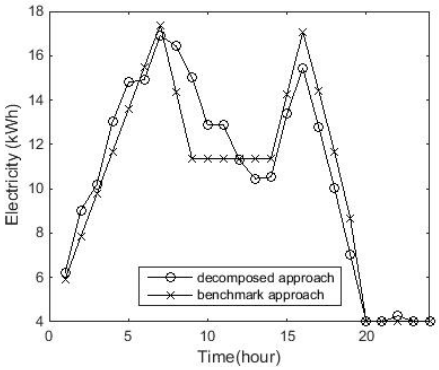

Fig. 6. The battery operations against 24 hours.

discharging/charging power (3kW), the battery operation at each time step can be derived and indicated in table I. Based on the operation of storage and heat pump, the total energy cost, *TC*, can be calculated as £6.73 from (11).

2) First scenario

The 2-hub system optimization problem is solved by the decomposed PSO method running on a 3.40 GHz Intel i5 quad core desktop with 8 GB of RAM. The procedures of implementing decomposed PSO is illustrated as follows:

1) A group of particles is generated, each particle contains each battery's charging and discharging energy over 24 time steps, which is randomly generated within the boundary set by optimization. Hence there are totally 48 variables contained in one particle. The charging and discharging energy in first three steps in the first particle is shown for example: 2.65 and 0.21, 1.24 and 0.11, 2.15, 0.02.
2) The SQP method is then applied to find a feasible point near the randomly generated point based on the battery constraints, in this case a feasible point indicates that the battery has to be either charging, discharging, or standby. The 6 variables in procedure 1 turns to be: 2.71 and 0, 1.21 and 0, 2.10 and 0.
3) The battery scheduling is then abstracted from the individual time step optimization, in that the charging and discharging power of the battery at each time step are regarded as extra energy exported/imported from/to the hub. Given the battery information and the constraints within the energy hub system, the 'interior-point' method is applied to optimally decide the variables over 24 time steps, such as the value of energy carrier injection to the hub, dispatch factor, etc. The total energy cost over whole time horizon can therefore be calculated, and regarded as the fitness score of the related particle.
4) The speed of each particle is generated based on equation (10), the PSO keeps updating particles' positions and speeds until the stopping criteria is met.

The optimization results of total energy cost over 24 hours are shown in table II over a range of different particle population sizes.

As shown from table II, the performance of the algorithm improves when the particle population increases. However, the optimization results do not consistently increase with increasing particle population due to the stochastic nature of PSO. The best result is £6.73, which demonstrates that the algorithm is capable of reaching very close to the global minimum for a highly-constrained, non-linear problem.

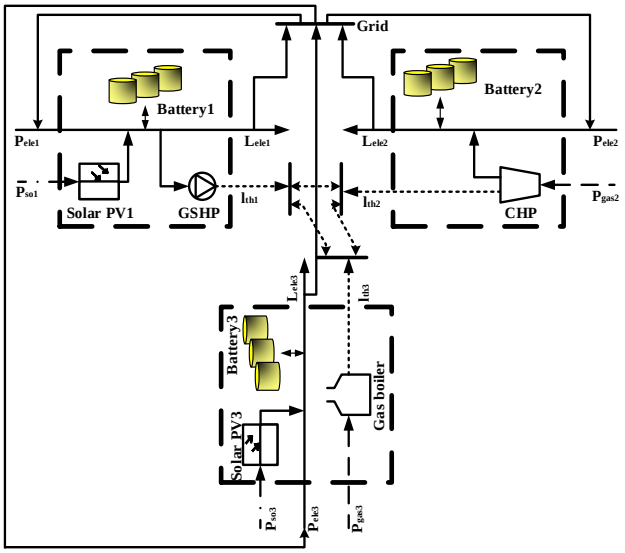

Fig. 7. Three-hub system with energy sharing available between hubs.

For comparison, when the storage is not present and energy sharing is unavailable between hubs, the energy demand for each hub can only be met with its own converters, and the total minimum energy cost is calculated as £7.84. When storage is not equipped with the system and energy sharing is available between hubs, the optimization problem is transformed to an optimal flow problem at each time step. The optimization can be solved by applying the 'interior-point' method, and the theoretical minimum energy cost is derived as £7.32. Compared with the 2-hub system without energy sharing and storage, the optimization achieves an energy saving of 14.14%.

To demonstrate the accuracy of decomposed-PSO, the optimal operation of the battery at each time step derived from a 30 particle optimization is compared with the battery operation derived from the benchmark approach, and is shown in Fig. 6. It can be observed that the optimized battery operations derived from the decomposed approach closely approximate to the operations obtained from the benchmark theoretical minimum.

B. Three-hub System

A three-hub system is presented and shown in Fig. 7. The three hubs respectively contain a battery with sizes of 5.3 kWh, 10.5 kWh and 21 kWh, the related battery parameters can be found in [25]. Different heating converters including GSHP, micro-CHP, and gas boiler are equipped in the three hubs. The CoP of GSHP is selected as 4, the constraint parameters of micro-CHP are adopted from [24, 32]. The efficiency of the gas boiler is non-linear against the gas input, and is illustrated in section II. The electricity load $L_{ele}(t)$ and heat load $L_{th}(t)$ for each hub are satisfied by optimally scheduling the utilization of all heating converters and batteries.

The gas price is assumed to be constant at £0.03 per kWh over all 24 time steps. The electricity price is varied every hour in this case to reflect the time-of-use electricity tariffs all

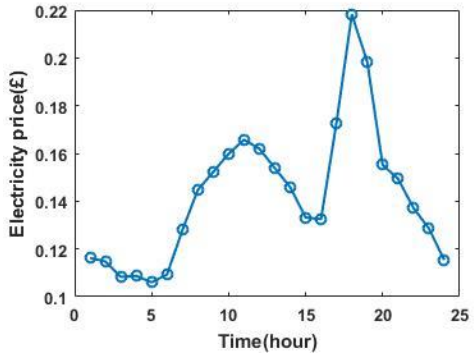

Fig. 8. The variant tariffs of electricity against 24 hours.

retailers will likely adopt in the near future. The variant electricity price against 24 hours is derived from [31] and shown in Fig. 8, with average half hourly tariffs used to produce an hourly pricing granularity. (These energy costs are typical in the UK at time of writing, but future prices will clearly yield different overall costs than the results shown in this paper.) The same method of modelling electricity demand and heat demand used in [31] is employed here. Additionally, the solar PV generations $P_{SO}(t)$ are simulated with the software [33]. To demonstrate the superiority of the decomposed approach, the conventional PSO is applied to solve this optimization problem. The comparison between the decomposed approach and conventional PSO is illustrated by convergence behaviour and computation time.

1) Second scenario

In this scenario, the performance between the conventional PSO and the decomposed approach in solving the optimization problem above is compared.

Since the time spent on conventional PSO increases massively with rising particle population size, a modest population of 10 particles was applied to both conventional PSO and decomposed approach to observe the convergence behaviour, and the comparison is shown in Fig. 9. The blue circles and the orange crosses represent the performance of applying conventional PSO and the decomposed approach respectively.

As indicated in Fig. 9, the objective function value by applying decomposed PSO plateaus from between 15 and 20 iterations onwards, for conventional PSO, the objective function value trends to flat around 35 iterations. Under the conservative stall generations (50) and stall tolerance settings (£0.000001), the conventional PSO optimization converges at the 162nd iteration after 8970 s, and the optimization result is £22.61. The decomposed approach converges at 143rd iteration after 121 s, and achieves a much improved optimization result of £9.30.

The optimized battery operations for hub 2, derived from two optimization methods, are shown in Fig. 10 in terms of battery SOC. The pink circles and orange crosses represent the battery SOC at each time step optimized by conventional PSO and decomposed PSO, and the blue dotted line indicates the electricity price variation over 24 time steps. From the perspective of optimally exploiting the storage to save energy cost, both of the two methods achieve the optimization by charging storage during the low tariff period and recharging

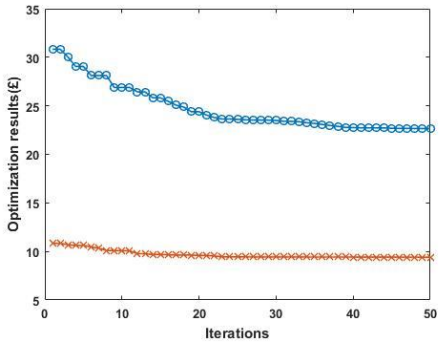

Fig. 9. Convergence behaviours of conventional PSO and decomposed approach.

during the high tariff period. It could be concluded from Fig. 10 that the electricity tariff experiences two peak values over 24 time steps. The two peak values appear at step 11 and step 18. Both of the optimization methods indicate that the storage is discharging since the first peak electricity price from step 9 to 10. Nevertheless, the storage operation derived from the decomposed approach discharges around the first peak electricity price from step 10 to 11, and then rapidly charges from step 11 to 18 to prepare for the second peak electricity price. With conventional PSO, the storage barely discharges at the first peak electricity price. Thus comparing with the conventional PSO, the decomposed approach can better optimize the storage operation and further reach the optimum. However, it could be derived from Fig. 10 that the battery scheduling operations derived from both optimization methods fail to fully discharge around the peak tariff period, which may lead to further cost saving. This is due to the low number of particles that degrades the performance of the optimization.

2) Impact of battery lifetime cost

To investigate the influence of battery lifetime cost in the objective function on battery scheduling, the optimization is run when considering battery lifetime and compared to when the battery lifetime consideration is omitted. 30 to 50 particles used in decomposed PSO reach a result very close to the global minimum for the 3-hub optimization based on extensive experimentation. Hence 50 particles are applied in the optimization. The SOC of three batteries over 24 time steps when considering battery lifetime and compared with excluding the battery lifetime in the objective function are shown in Fig. 11 and Fig. 12 respectively. The green, blue, and red lines

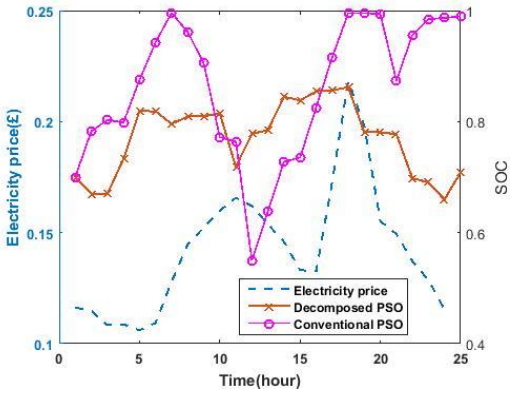

Fig. 10. The optimized battery operations by applying conventional PSO and decomposed approach.

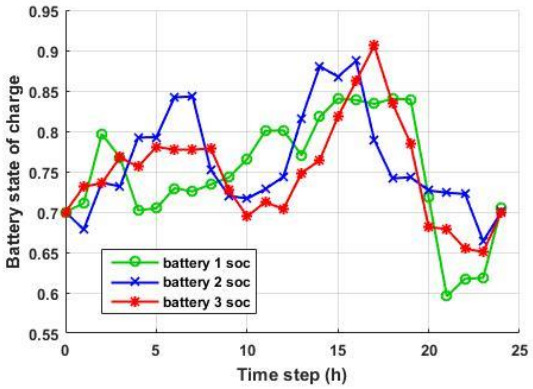

Fig. 11. Battery state of charge over 24 time steps derived from the optimization with the battery lifetime cost considered

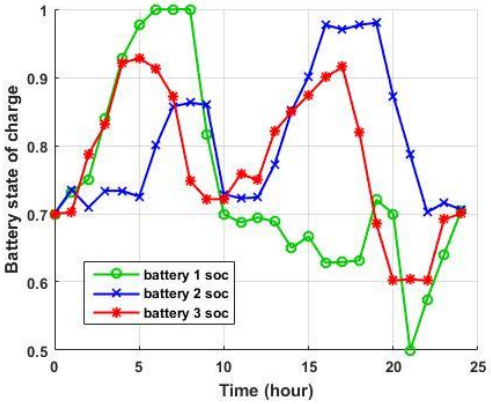

Fig. 12. Battery state of charge over 24 time steps derived from the optimization without considering the battery lifetime cost

represent the variation of SOC of battery in hub 1, 2, and 3 over 24 hours respectively.

The total energy costs for these two optimizations are £9.0268 and £9.0070, the battery lifetime costs are £0.0331 and £0.0728. Clearly when omitting the battery lifetime cost the batteries are exploited to yield more energy saving. However, the battery lifetime cost is higher, and thus the system total cost is higher (sum of energy cost and battery lifetime cost) at £9.0798, compared to £9.0599 when battery lifetime is considered. When the battery lifetime is not optimized, the variation of SOC is broader, for example, the battery in hub 1 even varies between 50% and 100%. When the battery lifetime is considered in the objective function, the SOC of three batteries all varies from approximately 60% to 90%. It may be concluded from the calculation of battery lifetime cost that the cost increases when the battery is operated during lower SOCs. Hence the battery is better operated at high SOCs to avoid unnecessary degradation of battery lifetime.

C. Applications

The optimization problem uses a fixed time step of one hour. To allow an online, receding time horizon implementation, the optimization for scheduling the system of energy hubs must be completed within the time step. Therefore, the size of the system of energy hubs that the decomposed approach is capable of optimizing within one hour is investigated. With the same modelling method applied, a 5-hub system and an 11-hub

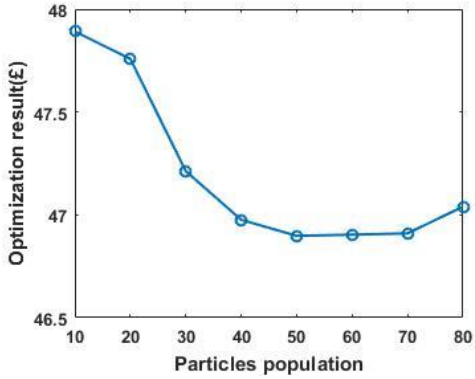

Fig. 13. Optimization results against different amount of particles

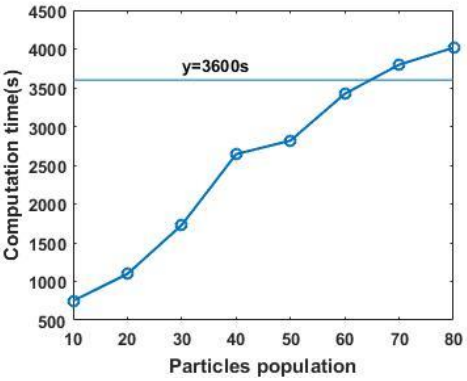

Fig. 14. Computation time against different amount of particles

system are simulated with the same level of complexity to the 3-hub system investigated in section V. The decomposed approach is applied with 30 particles to 3, 5, and 11 hub systems. The computation time for solving these three cases are 270 s, 779 s, and 1011 s respectively.

The decomposed approach was tested with different numbers of particles, for the 11-hub system, and the optimization results and computation time are shown in Fig. 13 and Fig. 14 respectively. In Fig. 14 ‘y=3600 s’ was drawn as a reference which indicates the time budget for a receding time horizon implementation with a time step of 1 hour.

It could be observed from Fig. 13 that the optimization results generally plateau at approximately £46.89 when the population of particles applied in PSO is 40. Increasing population size beyond this does not increase system benefit. In contrast, the computation time increases approximately linearly as the number of particles increases. The computation time of implementing PSO with 60 particles on this problem is 3421 s representing the best trade-off between computation time and performance for this particular system.

With a receding time horizon implementation, operations are calculated up to a certain time horizon, for which all load data is predicted in advance, but only the optimized operation for the next time step is implemented. In the next time step the time horizon is increased by one and the process is repeated. This makes the best use of load prediction data on the basis that the predicated data closer to the current time step is likely to be more accurate. On the other hand, a fixed time horizon approach may be used for larger multi-hub systems that are more computationally intensive to solve.

V. Conclusion

This paper presents a decomposed method that hybridises particle swarm optimization and the 'interior point' method to solve the optimal scheduling problem for a multi-energy hub system with the consideration of battery lifetime. For a 3 residential energy hub system, the utilization of battery varies from 60% to 90% to avoid unnecessary degradation of the battery lifetime, and the system thus benefits long term through increased battery lifetimes. Compared with the conventional PSO, the decomposed method can achieve a 58% greater energy saving for three-hub optimization with 98% saving of computation time. The optimization demonstrably achieves very near the global minimum. This method can be applied in a receding time horizon approach for solving a practical system of size around 10 hubs, always leveraging the most up to date load prediction. For a larger system with more storage technologies, a fixed time horizon approach can be used, or the time step may be increased or the time horizon reduced. From the view of energy management, the storage operation is more accurate when the predicted horizon is longer and generally speaking, the time step smaller, necessitating a trade-off between optimization performance and computation time. Alternatively, the computation time could be shortened using high performance hardware or cloud computing.

Appendix

A. Calculation of battery lifetime cost

The life loss of a battery $L_{loss}(t)$ over a certain time period t can be expressed as:

$$L_{loss}(t) = \frac{A_c(t)}{A_{total}} \quad \text{(A1)}$$

Where $A_c(t)$ is the effective cumulative Ah throughput during the use of battery and A_{total} is the total cumulative Ah throughput in the life cycle. The value of A_{total} is selected as $390Q$ effective Ah over its lifetime [25], which Q Ah is the capacity of a battery. $A_c(t)$ is formulated in (A2).

$$A_c(t) = \lambda_{soc} A'_c(t) \quad \text{(A2)}$$

λ_{soc} is the effective weighting factor. The relation between λ_{soc} and battery state of charge (SOC) is estimated as a linear formulation based on [25] and expressed in (A3).

$$\lambda_{soc} = \begin{cases} -1.5 \cdot SOC + 2.05 & if\ SOC \geq 50\% \\ 1.3 & if\ SOC < 50\% \end{cases} \quad \text{(A3)}$$

$A'_c(t)$ indicates the actual Ah throughput. Assuming the SOC of the battery varies from a to b in a certain time period, $A'_c(t)$ and $A_c(t)$ can be expressed in terms of a and b shown in (A4) and (A5) respectively.

$$A'_c(t) = (a - b) \times Q \quad \text{(A4)}$$

$$A_c(t) = \begin{cases} \int_b^a \lambda_{soc} dsoc \times A'_c(t) & if\ a \geq b \\ 0 & if\ a < b \end{cases} \quad \text{(A5)}$$

The life loss cost $C_{bl}(t)$ is calculated with (A6).

$$C_{bl}(t) = L_{loss}(t) C_{init-bat} \quad \text{(A6)}$$

$C_{init-bat}$ represents the initial investment cost of battery, and it is assumed to be 0.534 £/Ah [34] multiply by the battery capacity. The life loss cost can thus be calculated with (A1) to (A6).

B. Definition of convex problem

A convex optimization problem is defined by (A7) – (A9).

$$\text{Minimize} \quad f_0(x) \quad \text{(A7)}$$

$$\text{Subject to} \quad f_i(x) \leq b_i, \quad i = 1, \ldots, m \quad \text{(A8)}$$

Where functions $f_0, \ldots, f_m$: $R^n \to R$ are convex, i.e., satisfy

$$f_i(\alpha x_1 + (1-\alpha)x_2) \leq \alpha f_i(x_1) + (1-\alpha) f_i(x_2) \quad \text{(A9)}$$

for all $x_1, x_2 \in R^n$ and all $\alpha \in R, \alpha \geq 0$.

References

[1] S. Pazouki, and M. R. Haghifam, "Optimal planning and scheduling of energy hub in presence of wind, storage and demand response under uncertainty," *International Journal of Electrical Power & Energy Systems*, vol. 80, pp. 219-239, Sep, 2016.

[2] M. Geidl, and G. Andersson, "Optimal Power Flow of Multiple Energy Carriers," *Power Systems, IEEE Transactions on*, vol. 22, no. 1, pp. 145-155, 2007.

[3] M. Geidl, G. Koeppel, P. Favre-Perrod, B. Klockl, G. Andersson, and K. Frohlich, "Energy hubs for the future," *Ieee Power & Energy Magazine*, vol. 5, no. 1, pp. 24-30, Jan-Feb, 2007.

[4] F. Kienzle, P. Favre-Perrod, M. Arnold, and G. Andersson, "Multi-energy delivery infrastructures for the future." pp. 1-5.

[5] X. H. Guan, Z. B. Xu, and Q. S. Jia, "Energy-Efficient Buildings Facilitated by Microgrid," *Ieee Transactions on Smart Grid*, vol. 1, no. 3, pp. 243-252, Dec, 2010.

[6] M. Moeini-Aghtaie, A. Abbaspour, M. Fotuhi-Firuzabad, and E. Hajipour, "A Decomposed Solution to Multiple-Energy Carriers Optimal Power Flow," *Ieee Transactions on Power Systems*, vol. 29, no. 2, pp. 707-716, Mar, 2014.

[7] F. Adamek, M. Arnold, and G. Andersson, "On Decisive Storage Parameters for Minimizing Energy Supply Costs in Multicarrier Energy Systems," *Sustainable Energy, IEEE Transactions on*, vol. 5, no. 1, pp. 102-109, 2014.

[8] M. Arnold, R. R. Negenborn, G. Andersson, and B. De Schutter, "Model-Based Predictive Control Applied to Multi-Carrier Energy Systems," *2009 Ieee Power & Energy Society General Meeting, Vols 1-8*, pp. 4592-4599, 2009.

[9] A. Sheikhi, M. Rayati, S. Bahrami, and A. M. Ranjbar, "Integrated Demand Side Management Game in Smart Energy Hubs," *Ieee Transactions on Smart Grid*, vol. 6, no. 2, pp. 675-683, Mar, 2015.

[10] A. Sheikhi, M. Rayati, S. Bahrami, A. M. Ranjbar, and S. Sattari, "A cloud computing framework on demand side management game in smart energy hubs," *International Journal of Electrical Power & Energy Systems*, vol. 64, pp. 1007-1016, Jan, 2015.

[11] S. Bahrami, and A. Sheikhi, "From Demand Response in Smart Grid Toward Integrated Demand Response in Smart Energy Hub," *Ieee Transactions on Smart Grid*, vol. 7, no. 2, pp. 650-658, Mar, 2016.

[12] A. Sheikhi, S. Bahrami, and A. M. Ranjbar, "An autonomous demand response program for electricity and natural gas networks in smart energy hubs," *Energy*, vol. 89, pp. 490-499, Sep, 2015.

[13] F. Kamyab, and S. Bahrami, "Efficient operation of energy hubs in time-of-use and dynamic pricing electricity markets," *Energy*, vol. 106, pp. 343-355, Jul 1, 2016.

[14] A. Sheikhi, M. Rayati, S. Bahrami, and A. M. Ranjbar, "Demand Side Management in a group of Smart Energy Hubs as price anticipators; the game theoretical approach," *2015 IEEE Power & Energy Society Innovative Smart Grid Technologies Conference (ISGT)*, 2015.

[15] M. Schulze, and P. C. Del Granado, "Optimization Modeling in Energy Storage Applied to a Multi-Carrier System," *Ieee Power and Energy Society General Meeting 2010*, 2010.

[16] M. C. Bozchalui, S. AhsanHashmi, H. Hassen, C. A. Canizares, and K. Bhattacharya, "Optimal Operation of Residential Energy Hubs in Smart Grids," *Ieee Transactions on Smart Grid*, vol. 3, no. 4, pp. 1755-1766, Dec, 2012.

[17] B. Zhao, X. S. Zhang, J. Chen, C. S. Wang, and L. Guo, "Operation Optimization of Standalone Microgrids Considering Lifetime Characteristics of Battery Energy Storage System," *Ieee Transactions on Sustainable Energy*, vol. 4, no. 4, pp. 934-943, Oct, 2013.

[18] W. Ongsakul, and D. N. Vo, "Artificial Intelligence in Power System Optimization PREFACE," *Artificial Intelligence in Power System Optimization*, pp. V-V, 2013.

[19] T. Y. Lee, "Operating schedule of battery energy storage system in a time-of-use rate industrial user with wind turbine generators: A multipass iteration particle swarm optimization approach," *Ieee Transactions on Energy Conversion*, vol. 22, no. 3, pp. 774-782, Sep, 2007.

[20] M. A. A. Pedrasa, T. D. Spooner, and I. F. MacGill, "Coordinated Scheduling of Residential Distributed Energy Resources to Optimize Smart Home Energy Services," *Ieee Transactions on Smart Grid*, vol. 1, no. 2, pp. 134-143, Sep, 2010.

[21] F. Zhao, J. J. Si, and J. J. Wang, "Research on optimal schedule strategy for active distribution network using particle swarm optimization combined with bacterial foraging algorithm," *International Journal of Electrical Power & Energy Systems*, vol. 78, pp. 637-646, Jun, 2016.

[22] C. P. a. S. T. Liu, ""Performance of a commercial hot water boiler," U.S. Dept. Commerce Technol. Admin., Nat. Inst. Standards Technol., Gaithersburg, MD, USA, Tech. Rep. NISTIR 6226," 1998.

[23] M. E. Baster, "Modelling the performance of Air Source Heat Pump Systems," *Thesis, University of Strathclyde*, 2011.

[24] M. Houwing, R. R. Negenborn, and B. De Schutter, "Demand Response With Micro-CHP Systems," *Proceedings of the Ieee*, vol. 99, no. 1, pp. 200-213, Jan, 2011.

[25] D. P. Jenkins, J. Fletcher, and D. Kane, "Lifetime prediction and sizing of lead-acid batteries for microgeneration storage applications," *Iet Renewable Power Generation*, vol. 2, no. 3, pp. 191-200, Sep, 2008.

[26] J. Kennedy, and R. Eberhart, "Particle swarm optimization." pp. 1942-1948 vol.4.

[27] R. E. Perez, and K. Behdinan, "Particle swarm approach for structural design optimization," *Computers & Structures*, vol. 85, no. 19-20, pp. 1579-1588, Oct, 2007.

[28] S. Ebbesen, P. Kiwitz, and L. Guzzella, "A Generic Particle Swarm Optimization Matlab Function," *2012 American Control Conference (Acc)*, pp. 1519-1524, 2012.

[29] I. Richardson, M. Thomson, D. Infield, and C. Clifford, "Domestic electricity use: A high-resolution energy demand model," *Energy and Buildings*, vol. 42, no. 10, pp. 1878-1887, Oct, 2010.

[30] R. M. Yao, and K. Steemers, "A method of formulating energy load profile for domestic buildings in the UK," *Energy and Buildings*, vol. 37, no. 6, pp. 663-671, Jun, 2005.

[31] R. Li, Z. M. Wang, S. Le Blond, and F. R. Li, "Development of Time-of-Use Price by Clustering Techniques," *2014 Ieee Pes General Meeting - Conference & Exposition*, 2014.

[32] F. Kienzle, P. Ahcin, and G. Andersson, "Valuing Investments in Multi-Energy Conversion, Storage, and Demand-Side Management Systems Under Uncertainty," *Ieee Transactions on Sustainable Energy*, vol. 2, no. 2, pp. 194-202, Apr, 2011.

[33] "Photovoltaic Geographical Information System - Interactive Maps, [Online] Available: http://re.jrc.ec.europa.eu/pvgis/apps4/pvest.php#."

[34] T. P. Zhou, and W. Sun, "Optimization of Battery-Supercapacitor Hybrid Energy Storage Station in Wind/Solar Generation System," *Ieee Transactions on Sustainable Energy*, vol. 5, no. 2, pp. 408-415, Apr, 2014.